



## SIMULATION-BASED PREDICTING THE POSITION OF ROAD TANK EXPLOSIONS. PART II: A CASE STUDY

Egidijus Rytas Vaidogas<sup>1</sup>, Lina Linkutė<sup>2</sup>, Dainius Stulgys<sup>3</sup>

<sup>1,2</sup>*Dept of Occupational Safety and Fire Protection, Vilnius Gediminas Technical University, Saulėtekio al. 11, LT-10223 Vilnius, Lithuania*

<sup>3</sup>*Lithuanian Technology Platform on Industrial Safety; P.O. Box 2846, VACP, Gedimino pr. 7, LT-01008 Vilnius, Lithuania*

*E-mails: <sup>1</sup>erv@vgtu.lt (corresponding author); <sup>2</sup>lina.linkute@vgtu.lt; <sup>3</sup>dainius.stulgys@danis.lt*

*Submitted 14 June 2011; accepted 30 September 2011*

**Abstract.** A case study describing a simulation-based prediction of geometric characteristics of a road tank accident is presented. The case study evaluates the performance of the accident prediction model proposed in the first part of this study (Vaidogas *et al.* 2012). The prediction of accident characteristics is decomposed into three tasks: (i) prediction of the longitudinal rest position of the tank vehicle within the road segment under analysis; (ii) prediction of the transverse rest position with respect to road centreline; and (iii) prediction of the departure angle of the tank. These tasks are performed by applying stochastic (Monte Carlo) simulation. The results of the prediction are simulated samples of the geometric accident characteristics. These samples are considered to be input information for the assessment of risk posed by a potential explosion of tank vehicle vessel. In this case study, the potential targets of the explosion are three reservoirs built in the roadside territory. The case study presents and discusses in detail probabilistic models used for the simulation. It is stated that a considerable part of these models are chosen subjectively due to scarcity of circumstantial data on road tank accidents. The predictive Bayesian approach to risk assessment is used as a methodological basis of the simulation. Results of the simulation are intended to be utilised for increasing the safety of transportation of hazardous materials by road tanks.

**Keywords:** stochastic simulation, BLEVE, road tank, road accident, rest position, departure angle, roadside obstacle, risk, truncated distribution, predictive Bayesian approach.

### 1. Introduction

A transportation of hazardous materials by road tanks opens up a possibility of an accident which starts with a traffic accident and escalates into a boiling liquid expanding vapour explosion (BLEVE) (e.g., Bubbico, Marchini 2008). The effects of a BLEVE on vulnerable roadside objects can be assessed by a large number of deterministic and probabilistic models proposed in numerous publications (e.g., see the review given by Abbasi, T., Abbasi, S. 2007). An essential element of the estimation of risk to roadside property posed by BLEVEs is a prediction of the position and orientation of the tank car involved in traffic accident after it comes to a final stop and can explode.

Probabilistic models expressing the uncertainties related to position and orientation of the tank car after a traffic accident were proposed in the first part of this study (Vaidogas *et al.* 2012). The second part demonstrates how to apply these models to a stochastic simu-

lation of a tank rest position coordinates and departure angles. The simulation of these geometric characteristics can yield statistical samples which can be further used for assessing the risk to a vulnerable roadside object which can be damaged by a BLEVE. An application of methods of stochastic (Monte Carlo) simulation to traffic safety problems is a broad field with numerous publications (e.g., Waldeer 2003; Mitra, Washington 2007; Wang *et al.* 2009; El-Basyouny, Sayed 2009; Meng *et al.* 2010). However, these publications do not provide direct answers to the questions addressed in this case study.

The present paper uses symbols, nomenclature and acronyms introduced in the first part of the study (Vaidogas *et al.* 2012). The prime aim of the paper is to evaluate the performance of the accident prediction model proposed in the first part. The case study reveals what data and models are still necessary to accomplish an important part of transportation risk analysis related to precursors (initiators) of explosions on road.

## 2. The Site of an Accident Involving an Explosion on the Road

The proposed approach to the simulation of the position of a road tank accident will be illustrated by considering an oil transshipment facility built in the main seaport of Lithuania. The ‘target’ in this example is three cylindrical reservoirs which can be damaged by a tank explosion on a road with two 3 m lanes going along the perimeter of the facility (Fig. 1). The road has no gradient and the roadside territory is flat. Road tanks travel along the road in opposite directions with approximate relative frequencies 70% and 30%. Consequently, it is assumed that the probabilistic weights related to opposite lanes are  $\pi_1 = 0.7$  and  $\pi_2 = 0.3$ .

A schematic plan of the site under consideration is shown in Fig. 2a. The unsafe segment of the road is determined by the distance  $\Delta_{max}$  going from the centre of the 1st and 3rd reservoirs to the respective roadway edge. The distance  $\Delta_{max}$  was assumed to be equal to 125 m. This is a tentative value serving as an illustration. The distance  $\Delta_{max}$  was not specified by solving the optimisation problem given by Eq. (4) from the first part of this paper or by means of some other reasoning.

The road segment defined by  $\Delta_{max}$  was disaggregated into five zones with different roadside features. The 13 m and 2 m land strips bounding the edge of the travel lanes in the zones indicate that tank rest position may lie outside the road surface. The distance of 13 m is approximately equal to the typical length of a tank semi-trailer. Information of Zones 1 to 5 is summarised in Table 1.

The roadside territory of Zones 2 to 5 is bounded by densely growing trees on one roadside and the fence marking the perimeter of the facility on the op-



Fig. 1. The site of potential accident of a road tank in vicinity of reservoirs (obtained by using the Google Earth software)

posite roadside. It is assumed that the fence constitutes an unmovable obstacle to the tank vehicle and so the outermost rest positions  $y_{4L}$  and  $y_{4R}$  will be transverse distances from the road centreline to the fence minus half-width of the tank semi-trailer (1.25 m, say). It is also assumed that the tank vehicle can encroach into the forest territory on the opposite roadside and therefore the outermost rest positions  $y_{4L}$  and  $y_{4R}$  related to this side will be considered random quantities and modelled by the normal distribution  $N(5 \text{ m}, 0.25 \text{ m}^2)$ . Zone 1 is considered to have no obstacles on both sides of the road.

## 3. Simulation of the Longitudinal Rest Position

The probabilistic weights  $p_k$  ( $k = 1, 2, \dots, 5$ ) can be assigned to the zones in different ways. They include judgmental weighting often used for QRA (e.g., Aven 2003, 2009; Garrick 2008). However, as mentioned in Sec. 4.1, the weights  $p_k$  can also be specified by applying methods developed outside QRA, for instance, MCDM methods. A number of formal methods are suggested in the MCDM literature for specifying such weights as  $p_k$  in both crisp and fuzzy form (Triantaphyllou 2000; Sivilevičius, Maskeliūnaitė 2010; Vaidogas, Šakėnaitė 2010, 2011). These methods are used to elicit imprecise expert judgments and convert the judgments into the weights. However, these methods do not fully eliminate subjectivity in the specifying of  $p_k$ .

In the absence of any prior information, the weights  $p_k$  can be specified as the relative road surface areas of corresponding zones,  $A_k/A_{tot}$  (Table 1). However, one can argue that Zones 1, 3 and 4 are more prone to a vehicle accident than Zones 2 and 5. Therefore, the weights  $p_k$  should reflect not only the size of the zones but also this increased proneness.

Zone 1 includes a road intersection. Generally road intersections exhibit higher frequency of accidents as compared to other elements of roadway. For instance, Al-Ghamdi (2003) has found that the proportion of vehicle accidents at road intersections and non-intersections is approximately equal to 29% and 71%, respectively. As the stem of T-junction in Zone 1 is an access road to the facility and not a regular traffic artery, the proportion of 29% is too high for this intersection. We will use a somewhat reduced proportion expressed as the weight  $p_1$  equal to 0.25 (Table 1). Consequently, the sum of the remaining four weights must be equal to 0.75.

Zones 4 and 5 have unfavourable roadside features. It is well-known that characteristics of roadside features have a significant effect on frequency and severity of traffic accidents (e.g., Lee, Mannering 2002). The fence and trees standing close to the roadway edge in Zones 4 and 5 impair visibility and restrict avoidance manoeuvre, especially at the turn between the zones. The weights  $p_3$  and  $p_4$  can be assigned to Zones 3 and 4 by comparing these zones to Zones 2 and 5. The latter pair is less prone to vehicle accidents because there are no turns on the ends of Zones 2 and 5 and these zones have roadside obstacles only on one side. Consequently, the

sum  $p_3 + p_4$  should exceed the sum  $p_2 + p_5$ . The absence of the obstacles on one side of Zones 2 and 5 can be the reason for the choice  $(p_3 + p_4)/(p_2 + p_5) \geq 2$ . A possible distribution of the pairs of weights can be  $p_3 + p_4 = 0.5$  and  $p_2 + p_5 = 0.25$ . These aggregate weights can be distributed within the pairs  $p_3$  and  $p_4$  and  $p_2$  and  $p_5$  according to the relative road surface area  $A_k/A_{tot}$  given in Table 1:

$$p_{k(l)} = 0.25 A_{k(l)} / (A_k + A_l) \quad (k=2, l=5); \quad (1a)$$

$$p_{k(l)} = 0.5 A_{k(l)} / (A_k + A_l) \quad (k=3, l=4), \quad (1b)$$

where: the subscript  $k(l)$  indicates the weight  $p_k$  or  $p_l$  and the area  $A_k$  or  $A_l$  depending on which zone number

is considered. The calculation with Eqs. (1) yielded the weights  $p_2$  to  $p_5$  given in Table 1. The distribution of the weights  $p_k$  along the 280 m road segment is shown in Fig. 3a.

The longitudinal rest position  $y_3$  related to Zones 1, 2 and 5 was modelled by the uniform densities  $f_k(y_3)$  defined in Table 1 and illustrated in Fig. 3b. The piece-wise uniform density shown in Fig. 3c is related to the entire 280 m road segment. This density was constructed from the products  $p_k \times f_k(y_3)$ . It is the simplest model of the longitudinal rest position with respect to the 280 m road segment. Unfortunately, the density shown in Fig. 3c has unnatural jumps. Therefore, mixed densities were applied to Zones 2 to 5 to smooth out these jumps. The

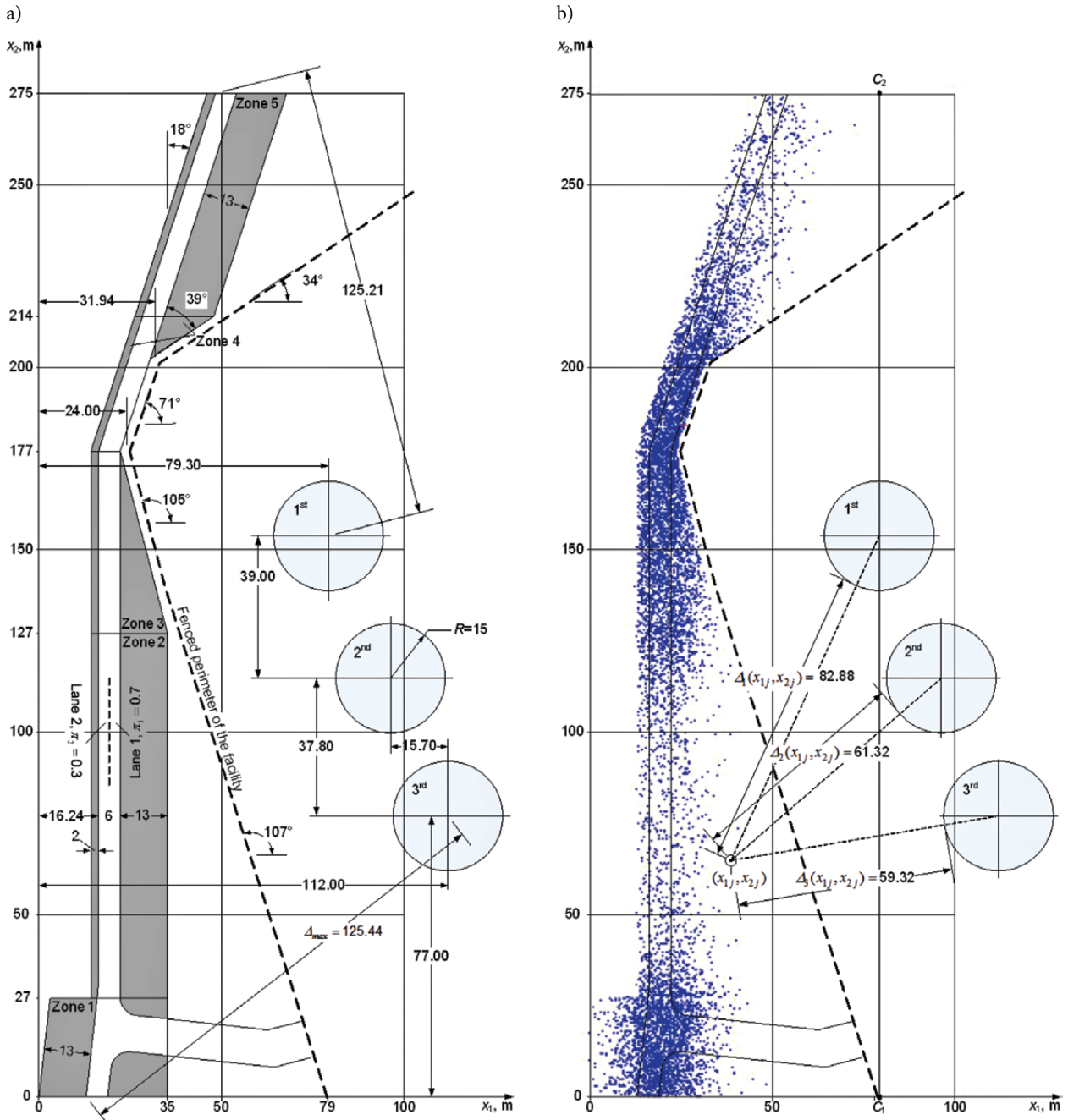


Fig. 2. Simulation of the road tank accident position: (a) scheme of the accident site; (b) scatter diagram of the simulated accident coordinates  $(x_{1j}, x_{2j})$  ( $j = 1, 2, \dots, N; N = 10\,000$ )

general expression of the mixed densities is given by:

$$f_k(y_3) = \omega f_{NU}(y_3) + (1-\omega) f_{UK}(y_3), \quad (2)$$

where:  $f_{NU}(\cdot)$  and  $f_{UK}(\cdot)$  are a non-uniform and uniform density, respectively. The non-uniform densities adapted to Zones 2 to 5 are explained in Table 1.

A power function distribution was used for smoothing out. This distribution is defined on a limited interval adaptable to the zone lengths  $l_k$  and allows a simple generation of random values by means of the inverse distribution function method (e.g., Evans *et al.* 2000). The triangular densities were applied to Zones 3 and 4.

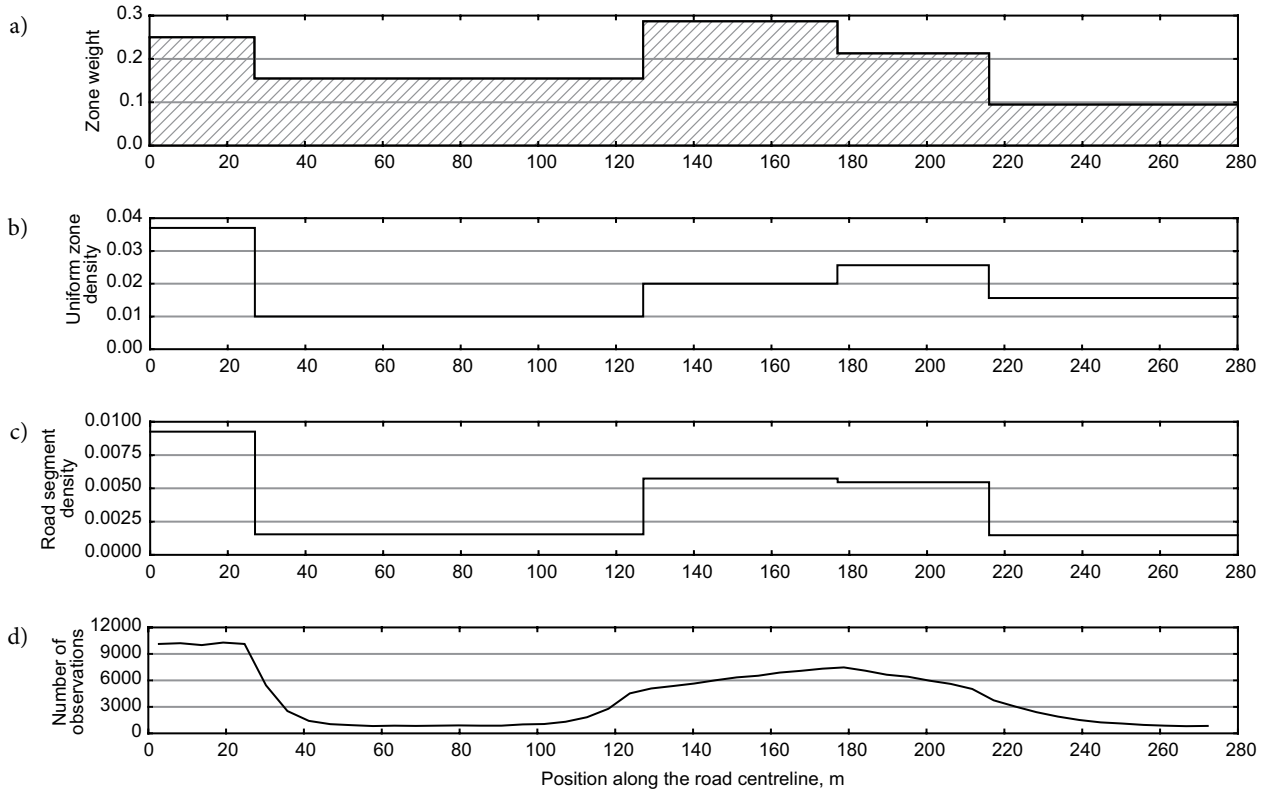


**Fig. 3.** Modelling the longitudinal rest position  $y_3$ : (a) the distribution of weights  $p_k$  assigned to Zones 1 to 5; (b) the uniform densities  $f_k(y_3)$  of  $y_3$  related to individual zones; (c) road segment density composed of the products  $p_k \times f_k(y_3)$ ; (d) the histogram of simulated values of  $y_{3j}$  obtained by smoothing the uniform densities as shown in Table 1 ( $j = 1, 2, \dots, N$ ;  $N = 2 \times 10^{-5}$ )

**Table 1.** Information about the zones of the road segment introduced in Figs 1 and 2

Zone number $k$	Length of zone, $l_k$ , m	Road surface area $A_k/A_{tot}^*$ , $m^2/m^2$	Probabilistic weight $p_k$	Probability density of the longitudinal rest position $y_3$
1	27	$162/1650 = 0.0982$	0.25	Uniform density: $f_{U1}(y_3) = 1/l_1$ ( $y_3 \in [0, l_1]$ )
2	100	$600/1650 = 0.3636$	0.155	Mixed power function** and uniform densities: $f_2(y_3) = 0.5\omega f_{PF}(y_3   \theta_1) + 0.5\omega f_{PF}(l_2 - y_3   \theta_2) + (1-\omega) f_{U2}(y_3)$ ( $y_3 \in [0, l_2]$ ), where $\omega = 0.5$ ; $\theta_1 = (12, l_2)$ ; $\theta_2 = (19, l_2)$ ; $f_{U2}(y_3) = 1/l_2$
3	50	$300/1650 = 0.1818$	0.287	Mixed triangular** and uniform densities: $f_3(y_3) = \omega f_T(y_3   \theta) + (1-\omega) f_{U3}(y_3)$ ( $y_3 \in [0, l_3]$ ), where $\omega = 0.2$ ; $\theta = (0, l_3, l_3)$ ; $f_{U3}(y_3) = 1/l_3$
4	39	$222/1650 = 0.1345$	0.213	Mixed triangular and uniform densities: $f_4(y_3) = \omega f_T(y_3   \theta) + (1-\omega) f_{U4}(y_3)$ ( $y_3 \in [0, l_4]$ ), where $\omega = 0.2$ ; $\theta = (0, 0, l_4)$ ; $f_{U4}(y_3) = 1/l_4$
5	61	$366/1650 = 0.2218$	0.095	Mixed power function and uniform densities: $f_5(y_3) = \omega f_{PF}(l_5 - y_3   \theta) + (1-\omega) f_{U5}(y_3)$ ( $y_3 \in [0, l_4]$ ), where $\omega = 0.5$ ; $\theta = (4, l_5)$ ; $f_{U5}(y_3) = 1/l_5$

**Notes:**  $*A_{tot} = 1650 m^2$ ;

\*\* $f_{PF}(\cdot)$  and  $f_T(\cdot)$  denote the power function density and triangular density, respectively (e.g., Evans *et al.* 2000)

They are used to express a potentially increased concentration of  $y_3$  values at the turn between the zones. The use of the mixed distributions of  $y_3$  allows to simulate the values of  $y_{3j}$  having a relatively smooth histogram (Fig. 3d).

#### 4. Simulation of the Transverse Rest Position

The sampling of the longitudinal rest position  $y_{3j}$  was followed by sampling of the transverse rest position  $y_{4j}$ . The values  $y_{4j}$  were generated from the logistic probability distributions fitted to the circumstantial data on road tank accidents (see Sec. 3.1 in Vaidogas et al. 2012). Each generation was preceded by a random choice among the lanes 1 and 2 with the respective weights  $\pi_1 = 0.7$  and  $\pi_2 = 0.3$  (Fig. 2a).

In Zone 1, the position  $y_{4j}$  was sampled from standard (non-truncated) logistic distributions Logistic(-3.52 m, 3.10 m) and Logistic(3.52 m, 3.10 m) related to the lanes 1 and 2, respectively. In Zones 2 to 5, the position  $y_{4j}$  was sampled from logistic distributions with the same parameters; however, these distributions were truncated on both sides (Fig. 4). The unmovable truncation points  $y_{4Rj}$  or  $y_{4Lj}$  determined by the position of the fence and related to the respective lanes 1 or 2 were computed for each simulated value of the longitudinal

rest position  $y_{3j}$ . The truncation points  $y_{4Rj}$  or  $y_{4Lj}$  related to the wood territory on the opposite road side were sampled from the normal distribution  $N(-5 \text{ m}, 0.25 \text{ m}^2)$  individually for each  $y_{3j}$ .

Fig. 4a shows the truncation interval  $[y_{4Lj}, y_{4Rj}] = [-4.75 \text{ m}, 10.04 \text{ m}]$  assigned to the longitudinal rest position  $y_{3j} = 38.7 \text{ m}$  simulated for Zone 3 and travel lane 1. The transverse rest position  $y_{4j} = 7.21 \text{ m}$  was sampled from the truncated Logistic(3.52 m, 3.10 m) with the density presented in Fig. 4a. The right truncation point  $y_{4Rj} = 10.04 \text{ m}$  is the distance between road centreline and fence minus 1.25 m (half-width of tank semi-trailer). The left truncation point  $y_{4Lj} = -4.75 \text{ m}$  was sampled from  $N(-5 \text{ m}, 0.25 \text{ m}^2)$  with the density shown in Fig. 4a. The truncation interval  $[y_{4Lj}, y_{4Rj}] = [8.23 \text{ m}, -5.38 \text{ m}]$  shown in Fig. 4b is related to the travel lane 2 in Zone 3. The value  $y_{4j} = -2.48$  was sampled from the truncated density defined on this interval and shown in Fig. 4b.

Sampling from the truncated logistic distributions was carried out by applying the inverse distribution function method (e.g., Gentle 2003). The following formula was used for the generation:

$$y_{4j} = F^{-1}(u_j(F(y_{4Rj}) - F(y_{4Lj})) + F(y_{4Lj}) | \theta_l), \quad (3)$$

where:  $l = 1$  or  $2$  depending on which lane is considered;  $F(\cdot)$  and  $F^{-1}(\cdot)$  are the direct and inverse distribution function of the logistic distribution, respectively.

The simulated pairs  $(y_{3j}, y_{4j})$  related to the coordinate systems of individual zones were transformed into the rest position  $(x_{1j}, x_{2j})$  in the coordinate system  $\{0; x_1, x_2\}$  shown in Fig. 2a. A scatter diagram drawn for 10 000 pairs  $(x_{1j}, x_{2j})$  and in Fig. 2b reveals the concentration of potential BLEVE accidents in the territory under study. However, the tank centre coordinates  $(x_{1j}, x_{2j})$  alone do not say anything about the orientation of the tank with respect to the road centreline and so the potential targets of BLEVE effects (reservoirs).

#### 5. Simulation of the Departure Angles

The simulation of the departure angles  $y_2$  was the most problematic part of this study. Values of the departure angle,  $y_{2j}$ , were sampled after sampling the pairs of the longitudinal and transverse rest position,  $(y_{3j}, y_{4j})$ . The sampling of  $y_{2j}$  was divided into two tasks:

- Task 1: sampling of  $y_{2j}$  in the case where the road tank is far from roadside obstacles and its rotation can not be restricted by them;
- Task 2: sampling of  $y_{2j}$  when the obstacles can or will restrict the tank rotation.

In the current simulation step  $j$ , the tasks were distinguished by considering the difference between transverse rest position  $y_{4j}$  and distance to a potential obstacle,  $y_{0j}$ . Task 1 was solved when difference  $|y_{0j} - y_{4j}|$  exceeded the half-length of tank semi-trailer (6.5 m in our case), whereas Task 2 took place when  $|y_{0j} - y_{4j}| \leq 6.5 \text{ m}$  (Fig. 5).

Task 1 was performed by a data-based sampling of the values  $y_{2j}$  from the empirical distribution of  $y_2$  in-

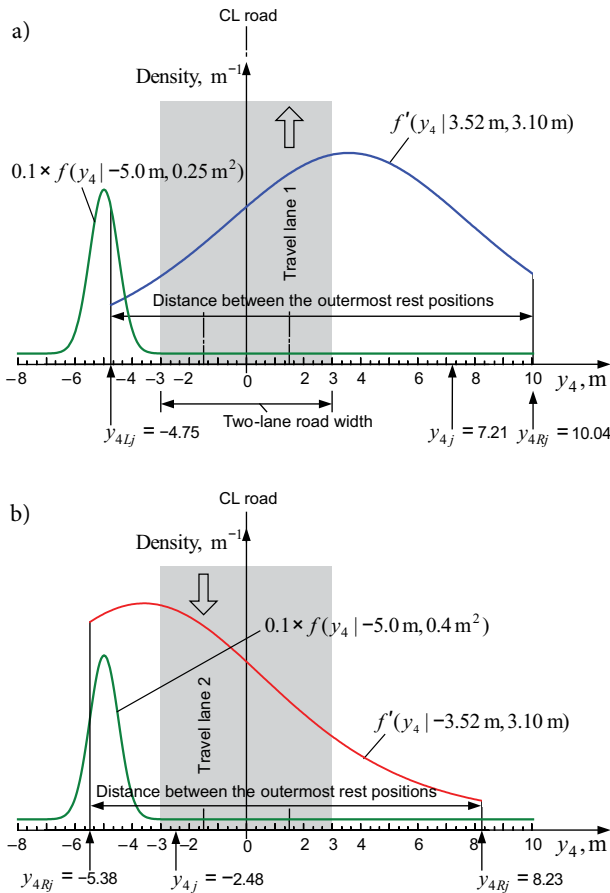


**Fig. 4.** Truncated logistic densities with the outermost rest positions  $[y_{4Lj}, y_{4Rj}]$  assigned to two values of the longitudinal rest position in Zone 3,  $y_{3j}$ : (a)  $y_{3j} = 38.7 \text{ m}$ ; (b)  $y_{3j} = -2.48 \text{ m}$

troduced in the first part of this study (Vaidogas *et al.* 2012). The weak stochastic dependence between transverse rest position  $y_4$  and departure angle  $y_2$  was expressed by a coefficient of correlation between  $y_4$  and  $y_2$  equal to 0.29. The values  $y_{2j}$  were sampled by means of the inverse transform method applied to a frequency polygon (e.g., Rubinstein, Melamed 1998). The stochastic dependence between the transverse rest position  $y_4$  and the departure angle  $y_2$  was regarded by applying the Thomson-Taylor data-based simulation (Gentle 2003).

Task 2 was much more difficult to solve due to lack (inaccessibility) of probabilistic models and circumstantial accident data allowing to simulate the departure angles in vicinity of roadside obstacles. Attempts to model an interaction of vehicles with roadside objects in detail are few and not directly applicable to a prediction of vehicle rotation angles (e.g., Ray 1999). Therefore, the simulation of  $y_2$  was underpinned by preliminary models which can be refined or replaced when new circumstantial information will be available.

The data-based sampling from the empirical distribution of  $y_2$  was extended by an approach similar to the acceptance-rejection method widely used in the field of stochastic simulation (e.g., Korn *et al.* 2010). The initially simulated angle  $y_{2j}$  was rejected and replaced by a maximum possible rotation angle  $y_{2j,max}$  in those simu-

lation steps where  $|y_{oj} - y_{4j}| \leq 6.5$  m (Fig. 5). The initial value  $y_{2j}$  was accepted or replaced by a new one using the simple rule:

$$y_{2j} = \begin{cases} y_{2j,max} & \text{if } y_{2j} \geq y_{2j,max} \\ y_{2j} & \text{otherwise,} \end{cases} \quad (4)$$

where:  $y_{2j,max}$  is the maximum possible rotation angle. The value of  $y_{2j,max}$  was determined by the position of the fence on one roadside or trees on the opposite roadside.

The computation of  $y_{2j,max}$  determined by the fence was straightforward. However, the restriction of the tank rotation by the wood on the opposite side of the road and so the simulation of  $y_{2j,max}$  was nontrivial. It was assumed that values of maximum outmost point of the tank,  $y_o$ , are strongly and negatively correlated with the maximum outmost position of the tank centre represented by the truncation points on the roadside planted with trees,  $y_{4R}$  or  $y_{4L}$ . The pairs  $(y_{4Lj}, y_{oj})$  and  $(y_{4Rj}, y_{oj})$  related to the respective travel lanes 1 and 2 were sampled from a bivariate normal distribution with the correlation coefficient equal to  $-0.9$ . Further parameters of this distribution are indicated in Fig. 6. The bivariate model assumes that the deeper is encroachment of the car into the wood the stronger is restriction of its rotation Fig. 6 illustrates the marginal densities of  $y_{4R}$  and  $y_o$  for the travel lane 2.

The simulation of the departure angles  $y_{2j}$  yielded the triples  $(y_{2j}, y_{3j}, y_{4j})$  which were transformed into the coordinates  $(x_{1j}, x_{2j}, x_{3j})$ . The latter tipples are visualized in Fig. 7 by means of arrows with the centre coordinates expressed by  $(x_{1j}, x_{2j})$  and the rotation angle given by  $x_{3j}$  ( $x_{3j} \in [0^\circ, 360^\circ]$ ).

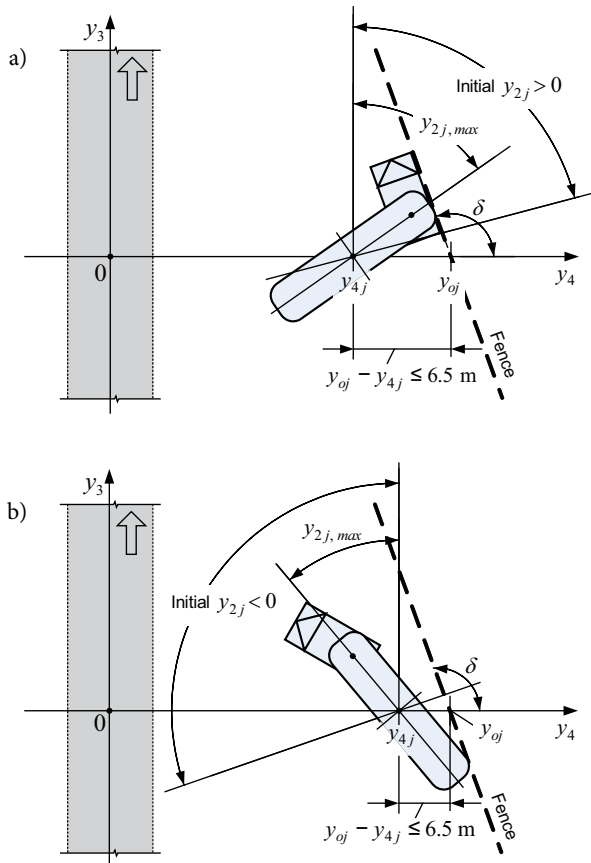


**Fig. 5.** Simulation of the departure angle  $y_2$  in vicinity of the fence represented by the dimensions  $y_{oj}$  and  $\delta$ :  
 (a) clock-wise rotation of the tank;  
 (b) counter clockwise rotation of the tank

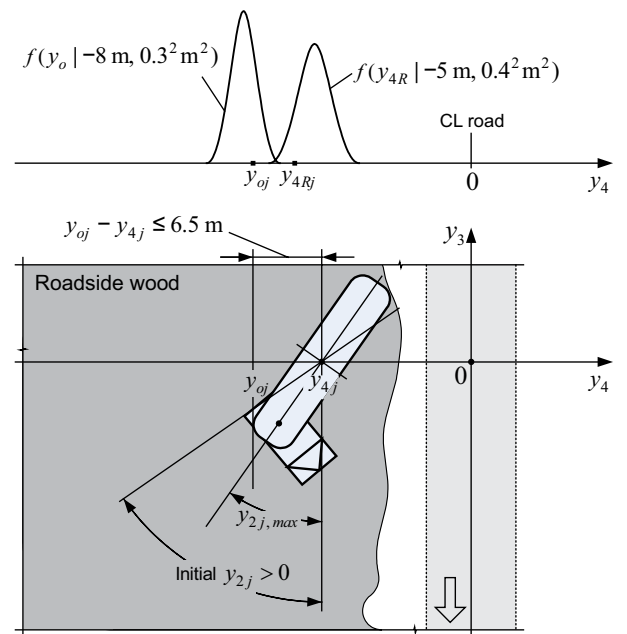


**Fig. 6.** Simulation of the departure angle  $y_2$  in the case of a road tank encroachment in the roadside wood with a clock-wise rotation with respect to travel direction

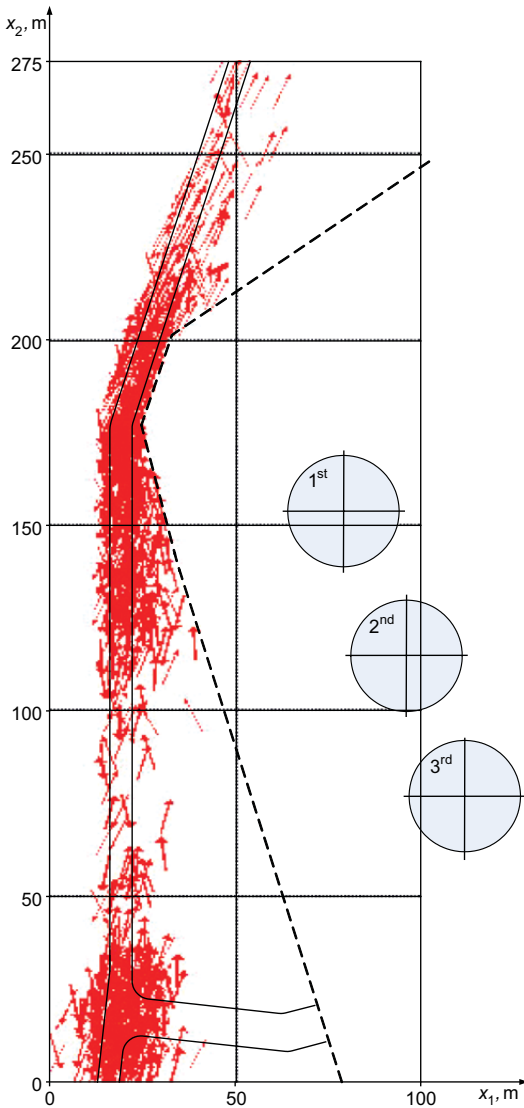


Fig. 7. A visualization of the simulated departure angle values  $x_{3j}$  shown by the arrows directed towards the front part of the tank vehicle ( $j = 1, 2, \dots, N$ ;  $N = 1000$ )

## 6. Results of the Simulation

The simulated accident coordinates  $(x_{1j}, x_{2j})$  can be easily transformed into the distances from the potential explosion centre to the targets (each of the three reservoirs)  $\Delta_r(x_{1j}, x_{2j})$  ( $r = 1, 2, 3$ ; see Fig. 2b). Probability distributions of these distances are key information necessary for the assessment of the potential damage from a BLEVE effects. The probability distributions can be fitted to the simulated samples:

$$\Delta_r = \{\Delta_r(x_{1j}, x_{2j}), j = 1, 2, \dots, N\}, \quad (5)$$

where:  $N$  is the number of simulations (the number of the pairs  $(x_{1j}, x_{2j})$ ). Descriptive measures of the samples  $\Delta_r$  generated with  $N = 10\,000$  are summarised in Table 2. Figs 8 a–c shows histograms of  $\Delta_r$  related to respective reservoirs.

In the case where the reservoirs are considered to be nominally identical and the damage event  $D$  given a

BLEVE event  $B$  is interpreted as maximum damage to one of them, an estimation of the conditional damage probability  $P(D | B)$  will require to establish a probability distribution of the minimum distance from the potential explosion centre to the closest reservoir. Such a distribution can be estimated from the simulated minimum distances:

$$\Delta_j = \min\{\Delta_r(x_{1j}, x_{2j}), r = 1, 2, 3\}. \quad (6)$$

A histogram of the sample:

$$\Delta_{min} = \{\Delta_j, j = 1, 2, \dots, N\} \quad (7)$$

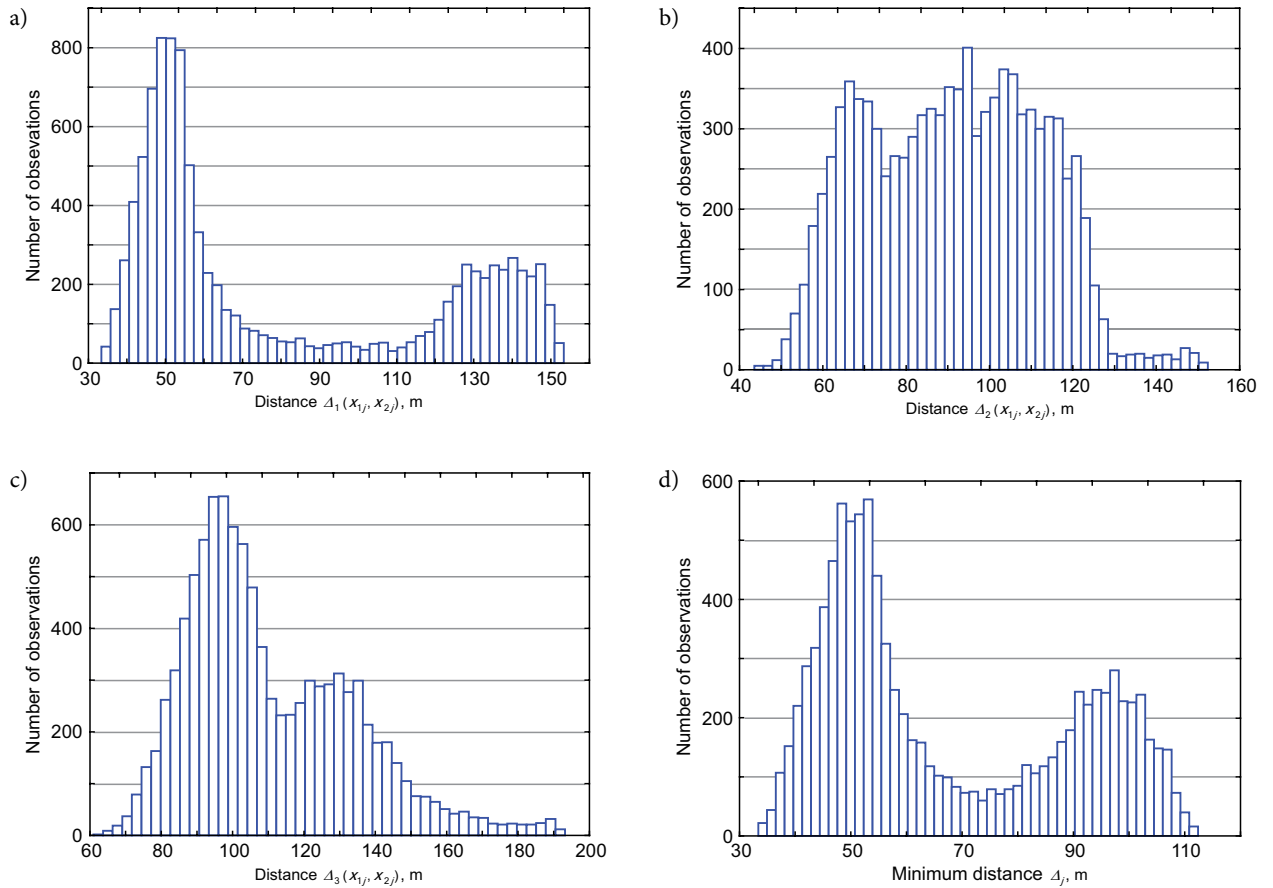
obtained with 10 000 simulated pairs  $(x_{1j}, x_{2j})$  is shown in Fig. 8d (i.e.,  $N = 10\,000$ ).

Table 2. Descriptive measures of the samples  $\Delta_r$  defined by Eq. (5) ( $r = 1, 2, 3$ ;  $N = 10\,000$ )

Measure	$r = 1$	$r = 2$	$r = 3$
Mean, m	79.8	91.4	110.5
Std. deviation, m	38.9	20.6	23.4
Minimum, m	33.4	43.6	58.3
Maximum, m	153.4	152.4	193.2
Skewness	0.660	0.095	0.830
Kurtosis	-1.285	-0.758	0.378
Std. skewness	26.9	3.89	33.9
Std. kurtosis	-26.2	-15.5	7.71

Fitting a probability distribution to the samples  $\Delta_r$  and  $\Delta_{min}$  is not a straightforward task because histograms of  $\Delta_r$  and  $\Delta_{min}$  are bimodal. However, the generation of the samples  $\Delta_r$  and  $\Delta_{min}$  does not require a big computational effort and the size of these samples,  $N$ , can be relatively large. In such a case, the samples  $\Delta_r$  and  $\Delta_{min}$  can be applied to the estimation of the damage probability  $P(D | B)$  directly, that is, without fitting a probability distribution to them (Vaidogas 2003, 2006, 2007, 2009; Vaidogas, Juocevičius 2007, 2008a, 2008b, 2009; Juocevičius, Vaidogas 2010).

Further substantial results of the simulation are the departure angles  $x_{3j}$ . They indicate the orientation of the tank axis during a potential vessel explosion. Projectiles from this explosion will probably follow the major tank axis although some scattering is possible (Birk 1996; Casal 2007). According to a statistical analysis of BLEVE accidents, approximately 60% of fragments are projected in an angular sector of  $60^\circ$  around the major axis of cylindrical tanks (Nguyen *et al.* 2009). A prediction of number, shape, velocity and trajectory of projectiles produced by BLEVEs of cylindrical vessels was addressed by many authors in both deterministic and probabilistic formats (e.g., CCPS 1994; Lees 1996; Vaidogas 2006; Abbasi, T., Abbasi, S. 2007; Gubinelli, Cozzani 2009; Mébarki *et al.* 2009). Such a prediction is beyond the scope of the present case study. However, the simulated directions  $x_{3j}$  allow to estimate at least the conditional probabilities that the tank axis will cross the reservoir  $r$  given a road tank accident ( $r = 1, 2, 3$ ). These probabili-



**Fig. 8.** Histograms of the simulated distances from explosion centre to reservoirs: (a, b, c) histograms of the samples  $\Delta_r$  ( $r = 1, 2, 3$ ) defined by Eq. (5); (d) histogram of the minimum distances  $\Delta_j$  ( $j = 1, 2, \dots, N$ ) (the sample  $\Delta_{min}$  is defined by Eq. (7)); ( $N = 10\ 000$ )

ties can be estimated by the relative crossing frequencies computed as  $N^{-1} \sum_{j=1}^N \mathbf{1}_{jr}$  with the binary variable:

$$\mathbf{1}_{jr} = \begin{cases} 1 & \text{if } x_{3j} \in [x_{jr}, \bar{x}_{jr}] \\ 0 & \text{otherwise,} \end{cases} \quad (8)$$

where:  $[x_{jr}, \bar{x}_{jr}]$  is the interval of  $x_3$  values which indicate crossing the reservoir  $r$  by the tank axis going through the point  $(x_{1j}, x_{2j})$  (Fig. 9).

A total of  $1 \times 10^5$  simulations yielded the following values of the crossing frequencies related to the respective reservoirs 1 to 3 shown in Figs 1 and 2: 0.03413, 0.01279, 0.00767. The frequency of non-crossing was correspondingly equal to 0.945. The crossing frequencies can be seen as conservative estimates of the likelihood of potential damage to the reservoirs by projectiles from a road tank BLEVE.

The above values of crossing frequencies can be explained by considering how often the major tank axis crossed a section  $[C_1, C_2]$  of the axis line of the 1<sup>st</sup> reservoir shown in Fig. 2b. The crossing frequency was equal to 0.1401. A histogram of crossing points within the interval  $[C_1, C_2]$  is given in Fig. 10. Most crossings occurred from Zones 4 and 5 which are closest to the 1<sup>st</sup> reservoir. The road in Zones 4 and 5 is not parallel to the reservoir axis and this is the main reason for

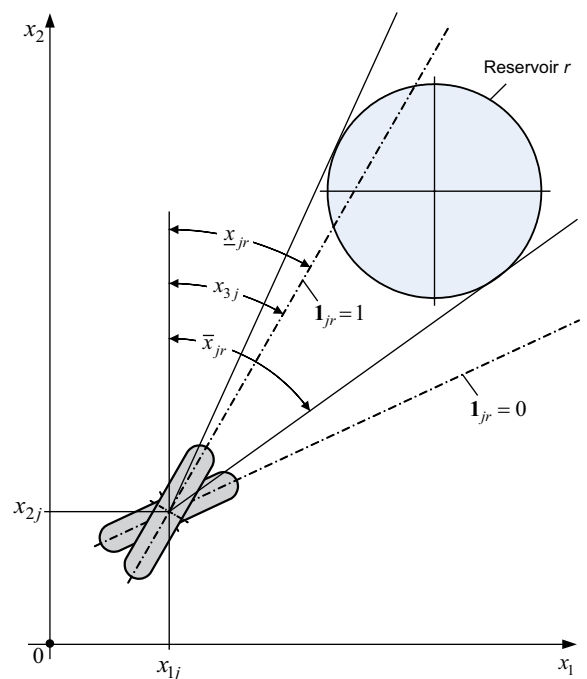


**Fig. 9.** A schematic illustration of the binary variable  $\mathbf{1}_{jr}$  indicating crossing or non-crossing of the reservoir  $r$  by an axis of tank car vessel

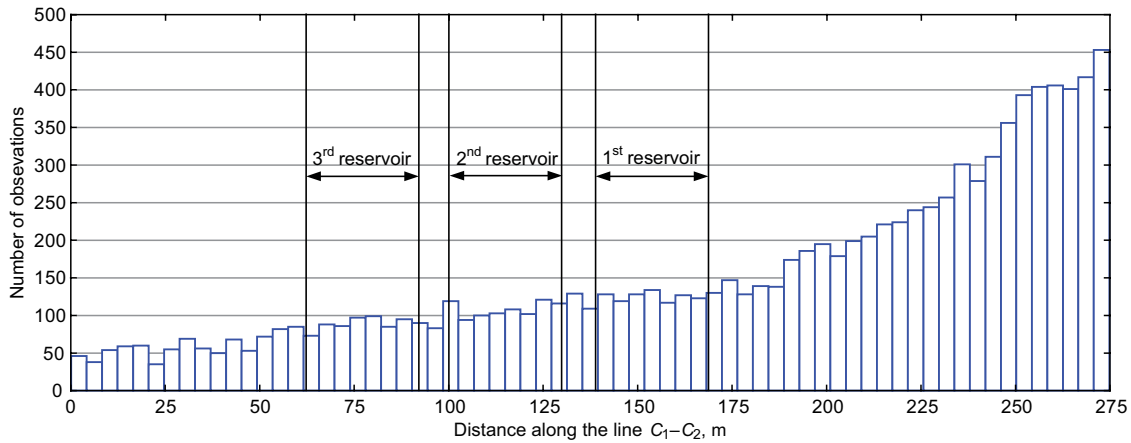


Fig. 10. A histogram of the points at which the major tank axis crossed the section  $[C_1, C_2]$  of the 1<sup>st</sup> reservoir axis shown in Fig. 2b

the increase of crossing frequencies. In many cases the tank axis running from Zones 4 and 5 crossed the first two or all three reservoirs at one time. In such cases the frequency was counted only for the 1<sup>st</sup> reservoir which was always closest to the tank and provided shelter for the 2<sup>nd</sup> and, sometimes, 3<sup>rd</sup> reservoirs. Therefore, the crossing frequency of the 1<sup>st</sup> reservoir is the largest one.

## 7. Conclusions

In this case study, a stochastic simulation of geometric characteristics of road tank accidents has been proposed. The simulation was based on data, models and algorithm presented in the first part of this paper (Vaidogas et al. 2012). The prime objective of the simulation was to generate information on the position and orientation of road tank vessels which can undergo a boiling liquid expanding vapour explosion (BLEVE). This information was expressed in the form of simulated statistical samples containing coordinates of tank rest position and the angle of tank vessel departure from the road centreline. Such information plays a crucial role in predicting thermal and mechanical effects of BLEVEs and assessing risk posed by BLEVEs to vulnerable roadside objects.

The case study used to evaluate the performance of the proposed accident prediction model highlighted several interesting results. Some of them count in favour of a simulation-based prediction of road tank accidents capable to escalate into BLEVEs; some results indicate that such a prediction will face certain problems.

First, a considerable body of information is required to develop a model for a stochastic accident simulation. One part of this information is hard historic data on past road tank accidents which not necessarily escalated into BLEVEs. However, another part of the information must be subjective experts' judgements. They will compensate the scarcity of hard historic data and this scarcity will be faced in most accident predictions.

Second, scarce historic data on past accidents can be combined with experts' judgements in the framework

of two basic approaches to a quantitative risk assessment (QRA). They are known as classical Bayesian and predictive Bayesian approaches to QRA. The latter approach is simpler and easier to apply to the case of road tank accidents. However, it should be remembered that the results produced by the predictive Bayesian approach are interpreted as completely subjective ones. They can be unacceptable or appear strange to users of risk analyses which have limited knowledge about possibilities and purposes of QRA.

Third, the prediction of position of road tank accidents and so potential explosions can be decomposed into three problems: (i) prediction of longitudinal rest position with respect to the road segment in the vicinity of a vulnerable roadside object; (ii) prediction of a transverse rest position; and (iii) prediction of departure angle relative to the road centreline. The proportion of the mathematical models backed by hard data and models chosen subjectively differs in these three problems. The largest amount of hard data is available to back the simulation of the transverse rest position of the tank and the angle of its departure from the road centreline. The most problematic in terms of data was the prediction of the longitudinal rest position. The specificity of the problem under investigation is that the segment of road infrastructure from which BLEVE can affect a roadside object is relatively small. Any history of road tank accidents for such small road segments will hardly be available in most cases. Therefore, the prediction of the longitudinal rest position will be based on subjectively chosen probabilistic models.

Finally, the simulation results presented in this paper should be seen only as an intermediate step of a QRA aimed at predicting consequences of a BLEVE on a road. However, the position and orientation of the tank car vessel at the instant of explosion is the key input information for the prediction of potential BLEVE damage. The simulation-based approach presented in this paper was intended to provide information for this important stage of transportation risk analysis.

## References

- Abbasi, T.; Abbasi, S. A. 2007. The boiling liquid expanding vapour explosion (BLEVE): mechanism, consequence assessment, management, *Journal of Hazardous Materials* 141(3): 489–519. <http://dx.doi.org/10.1016/j.jhazmat.2006.09.056>
- Al-Ghamdi, A. S. 2003. Analysis of traffic accidents at urban intersections in Riyadh, *Accident Analysis and Prevention* 35(5): 717–724. [http://dx.doi.org/10.1016/S0001-4575\(02\)00050-7](http://dx.doi.org/10.1016/S0001-4575(02)00050-7)
- Aven, T. 2003. *Foundations of Risk Analysis: A Knowledge and Decision-Oriented Perspective*. 1st edition. Wiley. 206 p.
- Aven, T. 2009. Perspectives on risk in a decision-making context – review and discussion, *Safety Science* 47(6): 798–806. <http://dx.doi.org/10.1016/j.ssci.2008.10.008>
- Birk, A. M. 1996. Hazards from propane BLEVEs: An update and proposal for emergency responders, *Journal of Loss Prevention in the Process Industries* 9(2): 173–181. [http://dx.doi.org/10.1016/0950-4230\(95\)00046-1](http://dx.doi.org/10.1016/0950-4230(95)00046-1)
- Bubbico, R.; Marchini, M. 2008. Assessment of an explosive LPG release accident: A case study, *Journal of Hazardous Materials* 155(3): 558–565. <http://dx.doi.org/10.1016/j.jhazmat.2007.11.097>
- Casal, J. 2007. *Evaluation of the Effects and Consequences of Major Accidents in Industrial Plants*. 1st edition. Elsevier Science. 378 p.
- CCPS 1994. *Guidelines for Evaluating the Characteristics of Vapor Cloud Explosions, Flash Fires, and BLEVEs*. 1st edition. Wiley-AIChE. 260 p.
- El-Basyouny, K.; Sayed, T. 2009. Accident prediction models with random corridor parameters, *Accident Analysis and Prevention* 41(5): 1118–1123. <http://dx.doi.org/10.1016/j.aap.2009.06.025>
- Evans, M.; Hastings, N.; Peacock, B. 2000. *Statistical Distributions*. 3rd edition. Wiley-Interscience. 221 p.
- Garrick, B. J. 2008. *Quantifying and Controlling Catastrophic Risks*. Academic Press. 376 p.
- Gentle, J. E. 2003. *Random Number Generation and Monte Carlo Methods*. 2nd edition. Springer. 264 p.
- Gubinelli, G.; Cozzani, V. 2009. Assessment of missile hazards: evaluation of the fragment number and drag factors, *Journal of Hazardous Materials* 161(1): 439–449. <http://dx.doi.org/10.1016/j.jhazmat.2008.03.116>
- Juocevičius, V.; Vaidogas, E. R. 2010. Effect of explosive loading on mechanical properties of concrete and reinforcing steel: towards developing a predictive model, *Mechanika* (1): 5–12.
- Korn, R.; Korn, E.; Kroisandt, G. 2010. *Monte Carlo Methods and Models in Finance and Insurance*. CRC Press. 484 p.
- Lee, J.; Mannering, F. 2002. Impact of roadside features on the frequency and severity of run-off-roadway accidents: an empirical analysis, *Accident Analysis and Prevention* 34(2): 149–161. [http://dx.doi.org/10.1016/S0001-4575\(01\)00009-4](http://dx.doi.org/10.1016/S0001-4575(01)00009-4)
- Lees, F. P. 1996. *Loss Prevention, Second Edition: Hazard Identification, Assessment and Control*. 2nd edition. Butterworth-Heinemann. 3000 p.
- Mébarki, A.; Mercier, F.; Nguyen, Q. B.; Ami Saada, R. 2009. Structural fragments and explosions in industrial facilities. Part I: Probabilistic description of the source terms, *Journal of Loss Prevention in the Process Industries* 22(4): 408–416. <http://dx.doi.org/10.1016/j.jlp.2009.02.006>
- Meng, Q.; Weng, J.; Qu, X. 2010. A probabilistic quantitative risk assessment model for the long-term work zone crashes, *Accident Analysis and Prevention* 42(6): 1866–1877. <http://dx.doi.org/10.1016/j.aap.2010.05.007>
- Mitra, S.; Washington, S. 2007. On the nature of over-dispersion in motor vehicle crash prediction models, *Accident Analysis and Prevention* 39(3): 459–468. <http://dx.doi.org/10.1016/j.aap.2006.08.002>
- Nguyen, Q. B.; Mebarki, A.; Ami Saada, R.; Mercier, F.; Reimeringer, M. 2009. Integrated probabilistic framework for domino effect and risk analysis, *Advances in Engineering Software* 40(9): 892–901. <http://dx.doi.org/10.1016/j.advengsoft.2009.01.002>
- Ray, M. H. 1999. Impact conditions in side-impact collisions with fixed roadside objects, *Accident Analysis and Prevention* 31(1–2): 21–30. [http://dx.doi.org/10.1016/S0001-4575\(98\)00041-4](http://dx.doi.org/10.1016/S0001-4575(98)00041-4)
- Rubinstein, R. Y.; Melamed, B. 1998. *Modern Simulation and Modeling*. Wiley-Interscience. 384 p.
- Sivilevičius, H.; Maskeliūnaitė, L. 2010. The criteria for identifying the quality of passengers' transportation by railway and their ranking using AHP method, *Transport* 25(4): 368–381. <http://dx.doi.org/10.3846/transport.2010.46>
- Triantaphyllou, E. 2000. *Multi-Criteria Decision Making Methods: A Comparative Study*. Springer. 320 p.
- Vaidogas, E. R. 2003. Accidental explosions: Bayesian uncertainty handling in assessing damage to structures, in *Proceedings of the 9th International Conference on Applications of Statistics and Probability in Civil Engineering*, July 6–9, 2003, San Francisco, CA, Eds. A. Der Kiureghian, S. Madanat, J. M. Pestana. Rotterdam: Milpress Science Publishers, Vol. 1, 191–198.
- Vaidogas, E. R. 2006. First step towards preventing losses due to mechanical damage from abnormal actions: Knowledge-based forecasting the actions, *Journal of Loss Prevention in the Process Industries* 19(5): 375–385. <http://dx.doi.org/10.1016/j.jlp.2005.10.002>
- Vaidogas, E. R. 2007. Handling uncertainties in structural fragility by means of the Bayesian bootstrap resampling, in *Proceedings of the 10th International Conference on Applications of Statistics and Probability in Civil Engineering (ICASP10)*, Tokyo, Japan, Jul 31 – Aug 03, 2007, Eds. J. Kanada, T. Takada, H. Furuta. London: Taylor & Francis (CD).
- Vaidogas, E. R. 2009. On applying sparse and uncertain information to estimating the probability of failure due to rare abnormal situations, *Information Technology and Control* 38(2): 135–146.
- Vaidogas, E. R.; Juocevičius, V. 2007. Assessing external threats to structures using limited statistical data: an approach based on data resampling, *Technological and Economic Development of Economy* 13(2): 170–175.
- Vaidogas, E. R.; Juocevičius, V. 2008a. Reliability of a timber structure exposed to fire: estimation using fragility function, *Mechanika* (5): 35–42.
- Vaidogas, E. R.; Juocevičius, V. 2008b. Sustainable development and major industrial accidents: the beneficial role of risk-oriented structural engineering, *Technological and Economic Development of Economy* 14(4): 612–627. <http://dx.doi.org/10.3846/1392-8619.2008.14.612-627>

- Vaidogas, E. R.; Juocevičius, V. 2009. Assessment of structures subjected to accidental actions using crisp and uncertain fragility functions, *Journal of Civil Engineering and Management* 15(1): 95–104.  
<http://dx.doi.org/10.3846/1392-3730.2009.15.95-104>
- Vaidogas, E. R.; Linkutė, L.; Stulgys, D. 2012. Simulation-based predicting the position of road tank explosions. Part I: data and models, *Transport* 27(1): 14–24.  
<http://dx.doi.org/10.3846/16484142.2012.663732>
- Vaidogas, E. R.; Šakėnaitė, J. 2010. Protecting built property against fire disasters: multi-attribute decision making with respect to fire risk, *International Journal of Strategic Property Management* 14(4): 391–407.  
<http://dx.doi.org/10.3846/ijspm.2010.29>
- Vaidogas, E. R.; Šakėnaitė, J. 2011. Multi-attribute decision-making in economics of fire protection, *Inžinerine Ekonomika – Engineering Economics* 22(3): 262–270.  
<http://dx.doi.org/10.5755/j01.ee.22.3.516>
- Waldeer, K. T. 2003. The direct simulation Monte Carlo method applied to a Boltzmann-like vehicular traffic flow model, *Computer Physics Communications* 156(1): 1–12.  
[http://dx.doi.org/10.1016/S0010-4655\(03\)00368-0](http://dx.doi.org/10.1016/S0010-4655(03)00368-0)
- Wang, C.; Quddus, M. A.; Ison, S. G. 2009. Impact of traffic congestion on road accidents: a spatial analysis of the M25 motorway in England, *Accident Analysis and Prevention* 41(4): 798–808. <http://dx.doi.org/10.1016/j.aap.2009.04.002>